Polymer 52 (2011) 2661–2666

Contents lists available at ScienceDirect

Polymer

journal homepage: www.elsevier.com/locate/polymer

Branch length distribution in TREF fractionated polyethylene

Ramnath Ramachandran [a], Gregory Beaucage [a,*], Douglas McFaddin [b], Jean Merrick-Mack [b], Vassilios Galiatsatos [b], Francis Mirabella [c]

[a] Department of Chemical and Materials Engineering, University of Cincinnati, 492 Rhodes Hall, M.L 0012, Cincinnati, OH 45221, USA
[b] Equistar Chemicals, LP, a LyondellBasell Company, Cincinnati Technology Center, 11530 Northlake Drive, Cincinnati, OH 45249, USA
[c] Mirabella Practical Consulting Solutions, Inc., 19155 Almadyde Ct., Port Charlotte, FL 33948-9602, USA

ARTICLE INFO

Article history:
Received 31 January 2011
Received in revised form
31 March 2011
Accepted 2 April 2011
Available online 8 April 2011

Keywords:
Polyethylene
Branching
Neutron scattering

ABSTRACT

Commercial polyethylene is typically heterogeneous in molecular weight as well as in molecular topology due to variability in catalyst systems and catalyst activity. Further, processing of polyethylene after polymerization may also result in changes to the structure. While quantification of molecular weight is routine using gel permeation chromatography (GPC); quantification of the heterogeneity in molecular topology and microstructure is more difficult. In this paper, a novel method is used to examine the structure and branch content of a linear low-density polyethylene (LLDPE). The method uses a scaling model to analyze small-angle neutron scattering (SANS) data from dilute solutions of a series of LLDPE fractions. The scaling approach quantifies short-chain and long-chain branch content in polymers concurrently, thereby illustrating the distribution of these branches in the polyethylene fractions. Additionally, new quantities such as the average long-chain branch length and hyperbranch content are measured to provide further insight into the structure of these polymers. LLDPE used in this study is fractionated using temperature rising elution fractionation (TREF). Results from the analysis of these fractions show evidence of long-chain branching in commercial LLDPE which could be partly attributed to post-synthesis processing conditions.

1. Introduction

The presence of branching in polyethylene has significant impact on its physical properties. Both short-chain and long-chain branching levels affect properties such as density, crystallinity, strength and processability [1–5]. In the production of commercial polyethylene, a variety of catalysts are used in order to obtain desired levels of branching. The presence of a mixture of active sites paired with the reaction conditions lead to distribution in molecular weight and branching in polyethylene. For example, Ziegler–Natta catalysts are known to result in heterogeneity in short-chain branched polyethylene [6]. Additional processing of polyethylene can affect the structure of the polymer as well. Common processing techniques such as extrusion, when air is not included, are thought to introduce low levels of long-chain branching in polyethylene that may result in unexpected physical properties [7,8]. Characterization methods such as gel permeation chromatography (GPC) are routinely used to measure the distribution in molecular weights. On the other hand, quantification of molecular topology and distribution in branching is more difficult. While GPC, along with nuclear magnetic resonance (NMR) spectroscopy, light scattering and rheological measurements are frequently used to measure branching, drawbacks posed by these techniques lead to incomprehensive quantification. For instance, GPC is ineffective in measuring low levels of branching; NMR is unable to distinguish effectively between short-chain and long-chain branches once the branch length exceeds six carbon atoms in length [9].

A novel scaling method [10–13] has been developed to comprehensively quantify branching in polyethylene [12,13]. The model has been applied successfully to characterize other ramified materials such as ceramic aggregates [10], proteins [14], hyperbranched polymers [15] and cyclics [16]. In the context of polyethylene the scaling model [10,11], when applied to small-angle neutron scattering (SANS) data, can quantify and distinguish between short-chain branching [12] and long-chain branching [13]; this allows for a complete analysis of branching. In this paper, the scaling model is applied to SANS data from a series of fractions of linear low-density polyethylene (LLDPE). Preparative temperature rising elution fractionation (pTREF) was utilized to fractionate LLDPE [17,18] into fractions that were characterized by other techniques.

* Corresponding author. Tel.: +1 513 556 3063; fax: +1 513 556 3443.
E-mail addresses: beaucag@uc.edu, gbeaucage@gmail.com (G. Beaucage).

0032-3861/$ – see front matter © 2011 Elsevier Ltd. All rights reserved.
doi:10.1016/j.polymer.2011.04.005

Linear low-density polyethylene is essentially a copolymer of ethylene with α-olefins such as butene, hexene and octene. Typically, commercial production of LLDPE utilizes heterogeneous multi-site Zeigler–Natta catalysts with varying comonomer concentration [6,19,20]. Consequently these LLDPEs have a broad distribution in molecular weight and short-chain branch (SCB) content. In order to effectively study the structure–property relationships of such heterogeneous resins, it is necessary to fractionate LLDPE into components with narrower distributions of molecular weight and SCB content. Temperature rising elution fractionation (TREF) has gained significant attention in this regard. TREF is a technique that fractionates a semi-crystalline polymer according to molecular structure that affects crystallinity. Since SCB content directly impacts crystallinity of polyethylene, TREF can fractionate LLDPE based on the SCB content [6,19–23].

2. Scaling model

The molecular structure of polyolefins such as polyethylene (PE) in dilute solution displays two levels: the average coil size R with mass-fractal dimension d_f, and an average substructural rod-like persistence unit of length[1] l_p or Kuhn length $l_k \approx 2l_p$ [24]. These structural features are observed in small-angle scattering patterns from polyethylene. The Unified Function [10,12,13,25,26] used in this article is useful in quantifying such structural features. Considering a short-circuit path through a branched structure, macromolecules exhibit an average tortuosity in this short-circuit path linked to the thermodynamic conditions and steric constraints. Branched macromolecules also display an average connectivity based on the branch content. The connectivity is invariant to changes in thermodynamic conditions. These two average features of branched chains can be described using a universal scaling model [10]. The scaling model has been useful in describing the structure and quantifying the topology of a variety of mass fractals [10–16].

For a polyethylene chain of end-to-end distance R and mass-fractal dimension d_f composed of z Kuhn steps of size l_k as shown in Fig. 1, the scaling model describes an average short-circuit path or minimum path p with mass-fractal dimension d_{min}. p and d_{min} account for the tortuosity in the chain. The connectivity of the polyethylene chain can be described by a connecting path s that is obtained by joining chain ends and branch points with straight lines. z, p and s can be related to the chain size R/l_k by,

$$z = \left(\frac{R}{l_k}\right)^{d_f}, p = \left(\frac{R}{l_k}\right)^{d_{min}} \text{ and } s = \left(\frac{R}{l_k}\right)^{c} \quad (1)$$

where c is the connectivity dimension. A scaling relationship between z, p and s can be expressed as [10,13],

$$z = p^c = s^{d_{min}} \quad (2)$$

Comparing Eqs. (1) and (2) yields $d_f = cd_{min}$. For regular objects such as spheres and discs that are completely connected and have no tortuosity, $d_f = c$ and $d_{min} = 1$. While d_{min} increases with tortuosity, c increases with increased connectivity. So, for linear polyethylene in a good solvent, $d_f = d_{min} \approx 5/3$ and 1. For branched polyethylene in a good solvent, $d_f > d_{min}$, $1 < c \le d_f$ and $1 \le d_{min} \le 5/3$. As described earlier [12,13], long-chain branching affects the overall size and scaling of the polyethylene chain, whereas short-chain branching affects the persistence length of polyethylene.

[1] Additionally, a dynamic size close to l_p called the packing length [3] can be defined which is not discussed here.

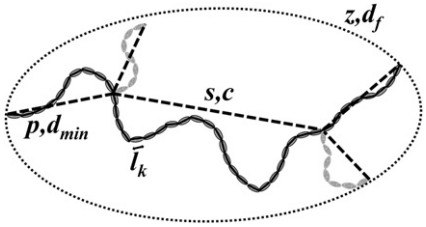

Fig. 1. Schematic of a branched polymer according to the scaling model. Each Kuhn step is represented by a bead. The polymer of mass-fractal dimension d_f is composed of z Kuhn steps of size l_k. The dark beads represent the minimum path p of dimension d_{min}. The lighter Kuhn steps symbolize the long-chain branches. The dotted lines represent the connective path of length s and dimension c.

The mole-fraction long-chain branch content can be obtained by [10,13],

$$\phi_{br} = \frac{z-p}{z} = 1 - z^{1/c-1} \quad (3)$$

The Unified Function [12,13,25,26] along with the scaling model [10] when applied to scattering data provides a plethora of information to describe the topology of branched polyethylene. For instance, the Unified Function in Eq (4) gives R_{g2}, G_2, B_2, G_1, B_1 and d_f.

$$I(q) = \left\{G_2 e^{-(q^2R_{g2}^2)/3} + B_2 e^{-(q^2R_{g1}^2)/3}\left(q_2^*\right)^{-d_{f2}}\right\} + \left\{G_1 e^{-(q^2R_{g1}^2)/3} + B_1\left(q_1^*\right)^{-1}\right\} \quad (4)$$

where $q_i^* = [q/\{erf(qkR_{gi}/\sqrt{6})\}^3]$ and $k \approx 1.06$.

The minimum dimension, d_{min}, is calculated from these parameters and is given by [10,13],

$$d_{min} = \frac{B_2 R_{g,2}^{d_f}}{C_p \Gamma\left(\frac{d_f}{2}\right) G_2} \quad (5)$$

where C_p is the polydispersity factor [12,13,27] and Γ is the gamma function. The weight-average number of Kuhn steps, z, is given by the ratio of G_2 over G_1 [10,12,26]. The connectivity dimension, c, is obtained from d_f/d_{min} as described in the scaling model. From the topological parameters obtained, an expression is derived [13] for the weight-average number of branch sites per chain, n_{br}, which is given by [13],

$$n_{br} = \left(\frac{z^{(5/2d_f - 3/2c) + (1-1/c)} - 1}{2}\right) \quad (6)$$

n_{br} is equivalent to the number of long-chain branches per chain that is obtained from NMR [13,28] for tri-functional branch points except that the NMR measurement is a number average. The mole-fraction branch content, ϕ_{br}, along with n_{br} are used to determine the weight-average long-chain branch length, z_{br}, from [13],

$$z_{br} = \frac{z\phi_{br}M_{Kuhn}}{n_{br}} \quad (7)$$

where M_{Kuhn} is the mass of one Kuhn step and assuming $f = 3$ (branch site functionality). For polyethylene, $M_{Kuhn} = 13.4\, l_k$, where M_{Kuhn} has units of g/mole and l_k has units of Å [13]. With respect to short-chain branched polyethylene with ethyl SCBs, it was previously shown that [12],

$$l_p = l_p^{\infty} - A\exp(-n_{SCB}/\tau) \quad (8)$$

where $l_p^{\infty} = 9.1 \pm 0.4$ Å is the persistence length of a fully short-chain branched polyethylene, n_{SCB} is the number of short-chain branches per 1000 carbon atoms, $A = 2.7 \pm 0.6$ Å and $\tau = 3.4 \pm 1.7$ for polyethylene. The LLDPE used in the current study (PE-1) was produced with 1-hexene comonomer resulting in butyl short-chain branches. The effect of butyl SCBs on the relationship described in Eq. (8) is described later in this article.

3. Experimental

3.1. Temperature rising elution fractionation

Temperature rising elution fractionation (TREF) is an established method that has proven valuable in the analysis of semi-crystalline polyolefins such as polyethylene and polypropylene [6,19–23]. TREF separates polymer molecules based on their melting point as controlled by short-chain branching. TREF has been particularly useful in analyzing conventional linear low-density polyethylene (LLDPE) grades produced with heterogeneous Ziegler–Natta catalysts due to their broad distributions in short-chain branch (SCB) content [6,19–21]. Basically, the TREF process consists of two steps: crystallization followed by elution. During the crystallization step, the polymer in dilute solution is cooled slowly (typically 5 °C/h and lower). Chains with low SCB content crystallize at higher temperatures. The elution step involves passing a good solvent through a column that is packed with the crystallized polymer mixture. The temperature of the solvent is increased step-wise, thereby eluting polymer fractions in the reverse order from which they precipitated. In preparative TREF, the fractions are collected at different elution temperature intervals for further analysis. A detailed review of TREF and the theory behind the separation has been discussed in the literature [23]. The weights of the fractions collected (98% recovery after fractionation) and their respective elution temperatures are listed in Table 1.

3.2. Small-angle neutron scattering

SANS was performed on dilute solutions of LLDPE in deuterated *p*-xylene, which is a good solvent for polyethylene at 125 °C. Butylhydroxytoluene (BHT) (500 ppm) was used as a stabilizer and dissolved in the solvent during sample preparation. BHT and deuterated *p*-xylene were purchased from Fisher Scientific. The samples were equilibrated at 125 °C for 2 h prior to the measurements to ensure complete dissolution of polyethylene. Additionally, the polymer solution was stirred by means of micro-magnetic stir bars to ensure proper mixing. 1 wt. % solutions were used, which is well below the overlap concentration [29] for all fractions. SANS experiments were carried out at NG-7 SANS [30] at the National Institute of Standards and Technology (NIST) Center for Neutron Research (NCNR), Gaithersburg and CG2 SANS in the High Flux Isotope Reactor (HFIR) at Oak Ridge National Laboratory (ORNL). Standard data correction procedures for transmission and incoherent scattering along with secondary standards were used to obtain $I(q)$ vs. q in absolute units [31]. Experimental runs took approximately 2 h per sample at both facilities.

4. Results and discussions

The corrected SANS data for the LLDPE fractions plotted in log-log plots of $I(q)$ vs (q) were fit to the Unified Function in Eq. (4) followed by the application of the scaling model. Fig. 2 shows the SANS data and the associated Unified fit for Frac 11. The molecular weight of PE-1 and the fractions were estimated from SANS using a method described by Boothroyd et al. [32]. The constant K in reference [32] accounts for the scattering contrast for the polymer in dilute deuterated solvent and is a property of the polymer, solvent and type of radiation. For polyethylene in deuterated p-xylene, the constant K was estimated to be 0.0012 mol cm^2 g^{-2}. NIST standard reference material 1484, a linear low-polydispersity standard, was utilized to determine K. Table 1 lists the quantities estimated from SANS and the scaling model that include persistence length, l_p, number of short-chain branches per 1000 carbon atoms, n_{SCB} (from NMR), mole-fraction long-chain branch content, φ_{br}, from Eq. (3), number of long-chain branch sites per chain, n_{br}, from Eq. (6), average long-chain branch length, z_{br}, from Eq. (7) and number of inner segments per chain, n_i, that was estimated as described in reference [13]. n_i is a measure of the hyperbranch content in a polymer chain [13]. The errors reported were propagated from the data.

4.1. Analysis of moments

It is known that scattering techniques like x-ray, light and neutron scattering measure the second moment of molecular weight (weight-average molecular weight, M_w) of polymers. In this paper, a number of quantities including M_w are measured from SANS. The analysis of the TREF fractions presents an opportunity to validate that these quantities measured are indeed weight-averaged quantities. The agreement between the SANS values and corresponding weight-average values, $\Sigma w_j X_j$, calculated by summing the contribution from individual fractions, in Table 2 is good and is persuasive evidence that the SANS values are indeed weight-averaged values. w_j is the ratio of the weight of each fraction to the total weight of the fractions collected. X_j represents the quantities measured from SANS (φ_{br}, n_{br}, z_{br}, n_i and l_p) for each fraction. Small discrepancies in Table 2 between the weight-

Table 1
SANS characterization of LLDPE fractions.

Sample	Weight, g	Elution temperature, °C	M_w, kg/mol	PDI	l_p, Å	n_{SCB} (NMR) #/1000 C	φ_{br}	n_{br}, #/chain	z_{br}, kg/mol	n_i, #/chain
PE-1	-	15	98	4.6	7.7 ± 0.5	18.5	0.127 ± 0.040	0.130 ± 0.020	17 ± 1.6	0.050 ± 0.020
Frac 1	1.04	30	13	6.3	8.9 ± 0.7	64.8	0.022 ± 0.001	0.007 ± 0.003	8 ± 0.8	0.007 ± 0.003
Frac 2	0.68	50	36	4.6	8.8 ± 0.6	46.1	0.028 ± 0.002	0.013 ± 0.003	10 ± 0.8	0.007 ± 0.003
Frac 3	1.26	70	46	3.5	8.5 ± 0.6	35.6	0.057 ± 0.002	0.038 ± 0.005	12 ± 1.3	0.012 ± 0.005
Frac 4	0.65	80	78	3.0	8.5 ± 0.5	28.5	0.057 ± 0.003	0.039 ± 0.006	11 ± 1.1	0.012 ± 0.006
Frac 5	1.57	85	83	2.7	8.2 ± 0.5	21.5	0.083 ± 0.003	0.074 ± 0.006	8 ± 0.8	0.010 ± 0.006
Frac 6	1.32	100	96	2.6	7.9 ± 0.5	17.5	0.129 ± 0.005	0.113 ± 0.008	12 ± 1.1	0.033 ± 0.008
Frac 7	1.62	110	108	2.5	7.0 ± 0.4	10.7	0.240 ± 0.010	0.149 ± 0.008	40 ± 1.5	0.149 ± 0.008
Frac 8	2.57	120	103	2.5	7.3 ± 0.5	5.9	0.153 ± 0.010	0.085 ± 0.007	9 ± 0.9	0.085 ± 0.007
Frac 9	1.43	125	118	1.9	7.0 ± 0.5	5.5	0.196 ± 0.040	0.122 ± 0.008	33 ± 1.5	0.110 ± 0.008
Frac 10	1.23	135	188	1.8	6.5 ± 0.4	3.9	0.295 ± 0.020	0.406 ± 0.050	60 ± 2.1	0.104 ± 0.053
Frac 11	1.28	150	245	1.7	6.6 ± 0.4	4.4	0.249 ± 0.008	0.155 ± 0.030	74 ± 2.3	0.155 ± 0.031

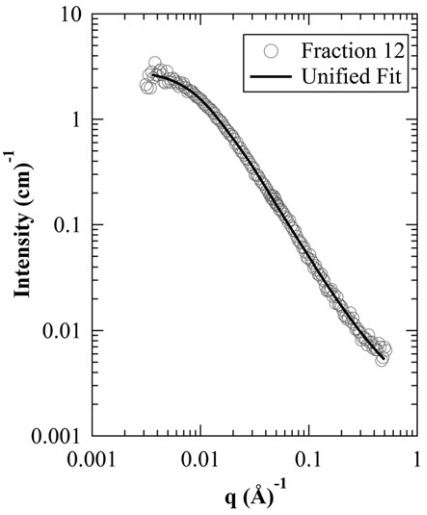

Fig. 2. SANS data from Fraction 11 fit to the Unified Function in Eq. (4). Data shown above was acquired at NIST.

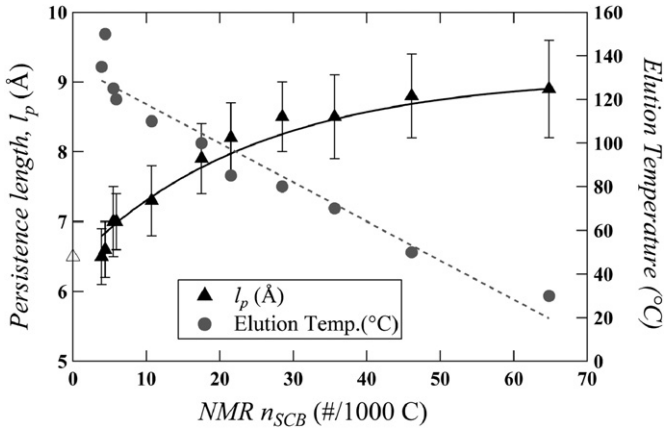

Fig. 3. Persistence length, l_p, from SANS (left axis) and TREF elution temperature (right axis) versus the number of SCBs per 1000 Carbon atoms from NMR. The open triangle represents linear polyethylene with no SCBs with $l_p = 6.5$ Å.

average values and the parent polymer values may be a result of incomplete recovery of the fractions from the TREF process.

4.2. Quantification of branching in LLDPE fractions

Fig. 3 plots the TREF elution temperature against the number of SCBs per 1000 carbon atoms from NMR. A linear increase in SCB content with decreasing elution temperature is observed. Fig. 3 also plots the persistence length, l_p, from SANS versus the NMR SCB content. In a previous study [12], the relationship between l_p and SCB content in Eq. (8) was obtained for ethyl short-chain branched polyethylene. In Eq. (8) A represents the range of change in the value of l_p with SCB content and $l_p^{\infty} = l_p^{0} + A$, where $l_p^{0} = 6.5$ Å for linear polyethylene with no short-chain branching. The SCB branch length is not expected to affect the maximum persistence length that can be obtained. In other words, the steric hindrance (that increases l_p) at maximum interference with chain motion remains approximately the same. Thus by fitting the data in Fig. 3 while keeping A and l_p^{∞} constant, τ is determined to be 24.6 ± 4.7. '$1/\tau$' is proportional to the rate at which l_p increases with SCB content [12]. The higher value of τ for butyl SCBs when compared to ethyl SCBs signifies a lesser effect of the number of SCBs on the persistence length. That is, a higher SCB content is needed to increase persistence length for butyl SCBs compared to ethyl SCBs. Hence, each butyl branch has a smaller steric effect on persistence length compared to each ethyl branch. This observation is contrary to the results seen in some simulation studies [33,34] based on bead and spring models that predict a larger steric effect with increasing SCB branch length. In the case of polyethylene, this discrepancy with simulation results may arise because SCB branch length can affect the local structure of the polymer in ways other than just sterically. For instance, ethyl short-chain branches could additionally introduce a helicity in the local structure analogous to the methyl side group in polypropylene, thereby sharply increasing the persistence length at low levels of branching. However, polyethylene with butyl branches might maintain a planar zigzag structure which results in a slower increase in persistence length with SCB density. Further, the distribution of SCBs in the backbone (blockiness) and the end group effects due to length of the backbone can also influence the rate of increase in persistence length.

For the LLDPE fractions, it is seen that the persistence length increases progressively with decreasing elution temperature thereby implying a decrease in SCB content with elution temperature. This observation corroborates the mechanism of the TREF process which fractionates the sample based on the SCB content. Fig. 4a illustrates this trend in a plot of number of SCBs per 1000 carbon atoms, n_{SCB} (right axis), against the weight-average molecular weight, M_w, of the fractions. Fig. 4a also plots the mole-fraction long-chain branch content, φ_{br} (left axis), against M_w. It is seen that the lower molecular weight fractions have extremely low amounts of LCBs (up to $\varphi_{br} = 0.1$) with the higher molecular weight fractions displaying LCB content of $\varphi_{br} \sim 0.2$–0.3. PE-1 contains smaller amounts of these high molecular weight fractions (about 25% by weight) and displays a low φ_{br} of 0.127.

Ziegler–Natta Ti-based LLDPE resins are not expected to contain LCB, since polymerization from such catalyst systems does not produce vinyl unsaturation via β-hydrogen abstraction, which is necessary to produce LCB [35,36]. This vinyl re-incorporation mechanism is seen as the reason behind the formation of LCBs in other catalyst systems such as metallocenes [37]. A different mechanism for introduction of long-chain branching in Ziegler–Natta systems has been reported by Reinking et al. [35]. Reinking et al. propose that LCBs may be introduced via C–H bond activation on the polymer backbone through σ-bond metathesis, followed by insertion of ethylene into the newly formed metal–carbon bond [35]. The SANS method used here has been successful in quantifying low amounts of LCBs in polyethylene previously [13]. The results reported in this article coupled with evidence reported previously [35] may suggest that Ti-based Ziegler–Natta catalysts possibly lead to low amounts of long-chain branching in some LLDPE.

An alternative explanation for the presence of long-chain branching in the higher fractions of the LLDPE studied here may be a result of the change in molecular structure during processing of polyethylene. The LLDPE polymer used in this study was post-processed. It has been previously hypothesized [7] that processing techniques such as extrusion, in the absence of air, introduce low levels of long-chain branching that result in unexpected rheological properties. Moreover, it is expected that LCBs are introduced preferentially in the higher molecular weight chains of

Table 2
Analysis of moments from SANS.

	M_w, kg/mol	φ_{br}	n_{br}, #/chain	z_{br}, kg/mol	n_i, #/chain	l_p, Å
PE-1	98	0.127	0.130	17	0.050	7.7
$\Sigma w_j X_j$	106	0.150	0.115	25	0.070	7.6

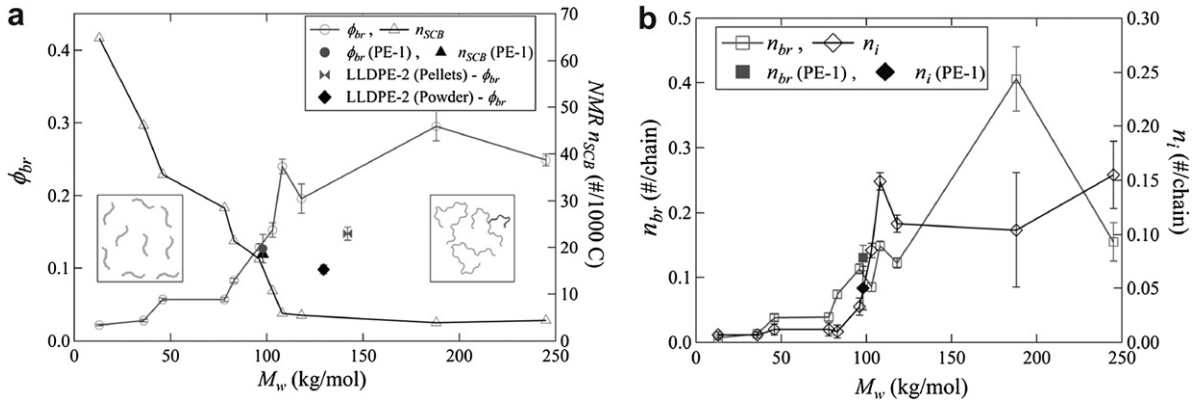

Fig. 4. (a) Plot of mole-fraction LCB content, φ_{br}, from Eq. (3) and number of SCBs per 1000 carbon atoms, n_{SCB}, *from NMR* against the weight-average molecular weight, M_w, obtained from SANS. (b) Plot of number of LCB sites per chain, n_{br}, from Eq. (6) and number of inner segments per chain, n_i, [13] versus M_w. The filled data points represent the corresponding values obtained for PE-1 that was fractionated by TREF.

the resin. The results here support this conjecture [7]. A pre-processed sample (straight from reactor) was not available for comparison for the LLDPE that was fractionated. But both pre-processed (powder) and post-processed (pellets) samples of a similar LLDPE (labeled LLDPE-2) were analyzed using the scaling approach. Fig. 4a plots the mole-fraction long-chain branch content, φ_{br}, of LLDPE-2. It is seen that the LCB content of the sample from the reactor (powder) is lower than the LCB content of the post-processed (pellets) sample. This observation indicates that processing could introduce long-chain branching in polyethylene.

Fig. 4b plots the number of long-chain branch sites per chain, n_{br}, and number of inner segments, n_i, versus M_w of the fractions. The method to obtain these quantities has been explained in detail previously [13]. For the LLDPE fractions, very low n_{br} and n_i are observed for the lower molecular weight fractions and slightly higher values for the higher molecular weight fractions. The filled data points in Fig. 4b represent the corresponding values for PE-1. Since PE-1 has smaller amounts of the high molecular weight fractions, low values for n_{br} and n_i are observed. As tabulated in Table 1, the average long-chain branch length, z_{br}, is nearly 3–7 times higher for the higher fractions when compared to lower fractions.

5. Conclusions

A novel scaling model was applied to small-angle neutron scattering data for dilute solutions of linear low-density polyethylene fractions that were obtained from preparative temperature rising elution fractionation. This method was able to differentiate and quantify the short-chain branch content (n_{SCB}) and long-chain branch content (φ_{br}) simultaneously for the fractions. Consequently, the branch length distribution in the LLDPE sample was investigated. In addition, the effect of the short-chain branch length on the structure of polyethylene was determined. While the results confirm that TREF separates the fraction in a polymer based on the SCB content, it also shows evidence of sparse amounts of long-chain branching that are usually undetected by traditional characterization techniques. For Ziegler–Natta systems, the results reported here are consistent with both a mechanism based on σ-bond metathesis for producing LCBs [35] and processing as a source of LCBs in polyethylene [7]. The number of LCB sites per chain (n_{br}), number of inner segments per chain (n_i) and average LCB length (z_{br}) were reported for the LLDPE fractions, providing further insight into the architectural distribution of these features in a commercial LLDPE resin.

Acknowledgements

This work was funded by Equistar Chemicals, LP and the University of Cincinnati Graduate School Distinguished Dissertation Completion Fellowship. This work utilized facilities supported in part by the National Science Foundation under Agreement No. DMR-0454672. We acknowledge the support of the National Institute of Standards and Technology (NIST), U.S. Department of Commerce, for providing the neutron research facilities used in this work. Research at Oak Ridge National Laboratory's High Flux Isotope Reactor was sponsored by the Scientific User Facilities Division, Office of Basic Energy Sciences, U.S. Department of Energy. We thank B. Hammouda and S. Kline at NIST and Y. Melnichenko at ORNL for their valuable support during the beamtime. We also thank M.K Reinking for useful comments.

References

[1] Garcia-Franco CA, Harrington BA, Lohse DJ. Macromolecules 2006;39(7):2710–7.
[2] Lohse DJ, Milner ST, Fetters LJ, Xenidou M, Hadjichristidis N, Mendelson RA, et al. Macromolecules 2002;35(8):3066–75.
[3] Fetters LJ, Lohse DJ, Richter D, Witten TA, Zirkel A. Macromolecules 1994;27(17):4639–47.
[4] Bishko G, McLeish TCB, Harlen OG, Larson RG. Phys Rev Lett 1997;79(12):2352–5.
[5] McLeish TCB, Larson RG. J Rheol 1998;42(1):81–110.
[6] Gabriel C, Lilge D. Polymer 2001;42(1):297–303.
[7] Epacher E, Fekete E, Gahleitner M, Pukanszky B. Polym Degrad Stabil 1999;63(3):499–507.
[8] Epacher E, Tolveth J, Stoll K, Pukanszky B. J Appl Polym Sci 1999;74(6):1596–605.
[9] Bovey FA. Pure Appl Chem 1982;54(3):559–68.
[10] Beaucage G. Phys Rev E 2004;70(3).
[11] Kulkarni AS, Beaucage G. J Polym Sci B Polym Phys 2006;44(10):1395–405.
[12] Ramachandran R, Beaucage G, Kulkarni AS, McFaddin D, Merrick-Mack J, Galiatsatos V. Macromolecules 2008;41(24):9802–6.
[13] Ramachandran R, Beaucage G, Kulkarni AS, McFaddin D, Merrick-Mack J, Galiatsatos V. Macromolecules 2009;42(13):4746–50.
[14] Beaucage G. Biophys J 2008;95(2):503–9.
[15] Kulkarni AS, Beaucage G. Macromol Rapid Commun 2007;28(12):1312–6.
[16] Beaucage G, Kulkarni AS. Macromolecules 2010;43(1):532–7.
[17] Zhang M, Lynch DT, Wanke SE. Polymer 2001;42(7):3067–75.
[18] Defoor F, Groeninckx G, Schouterden P, Vanderheijden B. Polymer 1992;33(18):3878–83.
[19] Soares JBP, Hamielec AE. Polymer 1995;36(8):1639–54.
[20] Usami T, Gotoh Y, Takayama S. Macromolecules 1986;19(11):2722–6.
[21] Mirabella FM, Ford EA. J Polym Sci B Polym Phys 1987;25(4):777–90.
[22] Mirabella FM. J Liquid Chromatogr 1994;17(14–15):3201–19.
[23] Wild L, Glöckner G. Temperature rising elution fractionation. In: Advances in polymer science, vol. 98. Berlin: Springer; 1991. pp. 1–47.
[24] Doi M, See H. Introduction to polymer physics. Clarendon Press; 1996.
[25] Beaucage G. J Appl Crystallogr 1995;28:717–28.
[26] Beaucage G. J Appl Crystallogr 1996;29:134–46.
[27] Sorensen CM, Wang GM. Phys Rev E 1999;60(6):7143–8.

[28] Costeux S, Wood-Adams P, Beigzadeh D. Macromolecules 2002;35(7):2514–28.
[29] Murase H, Kume T, Hashimoto T, Ohta Y, Mizukami T. Macromolecules 1995;28(23):7724–9.
[30] Glinka CJ, Barker JG, Hammouda B, Krueger S, Moyer JJ, Orts WJ. J Appl Crystallogr 1998;31:430–45.
[31] Kline SR. J Appl Crystallogr 2006;39:895–900.
[32] Boothroyd AT, Squires GL, Fetters LJ, Rennie AR, Horton JC, Devallera A. Macromolecules 1989;22(7):3130–7.
[33] Elli S, Ganazzoli F, Timoshenko EG, Kuznetsov YA, Connolly R. J Chem Phys 2004;120(13):6257–67.
[34] Connolly R, Bellesia G, Timoshenko EG, Kuznetsov YA, Elli S, Ganazzoli F. Macromolecules 2005;38(12):5288–99.
[35] Reinking MK, Orf G, McFaddin D. J Polym Sci A Polym Chem 1998;36(16):2889–98.
[36] DesLauriers PJ, Tso C, Yu Y, Rohlfing DL, McDaniel MP. Appl Catal A Gen 2010;388(1–2):102–12.
[37] Shaffer WKA, Ray WH. J Appl Polym Sci 1997;65(6):1053–80.